Ex Vivo and in Vivo Evaluation of Dodecaborate-Based Clusters Encapsulated in Ferumoxytol Nanoparticles

Nicholas A. Bernier[a], James Teh[b], Derek Reichel[b], Joanne L. Zahorsky-Reeves[c], J. Manuel Perez[b,d,e,†,], Alexander M. Spokoyny[a,f,*]*

[a]Department of Chemistry and Biochemistry, University of California, Los Angeles, CA 90095, USA

[b]Department of Neurosurgery, Cedars-Sinai Medical Center, Los Angeles, CA 90048, USA

[c]Division of Lab Animal Medicine, David Geffen School of Medicine, University of California, Los Angeles, CA 90095, USA

[d]Samuel Oschin Comprehensive Cancer Institute, Cedars-Sinai Medical Center, Los Angeles, CA 90048, USA

[e]Biomedical Imaging Research Institute, Cedars-Sinai Medical Center, Los Angeles, CA 90048, USA

[f]California NanoSystems Institute (CNSI), University of California, Los Angeles, California 90095, USA

KEYWORDS Host-Guest, Boron Cluster, Dodecaborate, Ferumoxytol, Nanoparticles, Biodistribution

Abstract

Host-guest interactions represent a growing research area with recent work demonstrating an ability to chemically manipulate both host molecules as well as guest molecules to vary the type and strength of bonding. Much less is known about the interactions of guest molecules and hybrid materials containing similar chemical features to typical macrocyclic hosts. This work uses in vitro and in vivo kinetic analyses to investigate the interaction of *closo*-dodecahydrododecaborate derivatives with ferumoxytol, an iron oxide nanoparticle with a carboxylated dextran coating. We find that several boron cluster derivatives can become encapsulated into ferumoxytol and the lack of pH dependence in these interactions suggests that ion pairing, hydrophobic/hydrophilic, or hydrogen bonding are not the driving force for encapsulation in this system. Biodistribution experiments in BALB/c mice show that this system is nontoxic at the reported dosage and demonstrate that encapsulation of dodecaborate-based clusters in ferumoxytol can alter the biodistribution of guest molecules.

Introduction

Host-guest interactions are ubiquitous in both biological and synthetic systems.[1] Over the past several decades, chemists have developed numerous powerful abiotic systems featuring modular and programmable binding affinities through intricate molecular design.[2] Boron clusters represent an emerging class of guest molecules capable of binding to a wide variety of both natural and synthetic macrocyclic hosts (Figure 1).[3] While many host-guest complexes are stabilized through a combination of hydrogen bonding and/or hydrophobic/hydrophilic interactions, research on boron-rich compounds and cyclodextrins currently suggests that chaotropism can be an important factor in these particular systems.[4-5] While macromolecules such as cyclodextrins and cucurbiturils[6] have been used to probe interactions with different boron cluster guests, much less is known about their noncovalent interactions with polymeric matrices containing similar local chemical structure of well-defined macromolecular hosts.[7] Recently, Li and coworkers used ion pairing interactions to noncovalently incorporate boron clusters into polymeric nanoparticles.[7] In this example, positively charged guanidinium functional groups appended to a polymer interact with negatively charged dodecaborate anions. Overall, further understanding and expanding the repertoire of the available noncovalent interactions that can be used to construct hybrid materials with boron clusters and polymers is needed.

Ferumoxytol (FMX) is a commercially available, FDA-approved hybrid nanoparticle formulation with an iron oxide core coated with a carboxylated dextran polymer.[8] Recent reports have shown that iron oxide nanoparticles, such as FMX, are capable of efficiently encapsulating several drug compounds that can be subsequently released *in vivo*.[9-12] Given the chemical similarity of cyclodextrins to the dextran polymer in FMX, we hypothesized that these nanoparticles could be used to encapsulate boron-rich compounds which would potentially

associate strongly with the FMX matrix (Figure 1). Importantly, the zeta potential of FMX is negative (-24 mV)[8B] which suggests that forces other than ion pairing would likely drive the incorporation of negatively charged dodecaborate anions into FMX. Specifically, in this work, we report the successful encapsulation and kinetic analyses of the subsequent release of 13 dodecaborate-based guests from FMX. While ^{11}B NMR spectroscopy showed evidence of encapsulation, it proved much less useful in determining the stability of each encapsulated system. Dynamic dialysis was therefore used to further interrogate release rate constants between various derivatives of boron clusters encapsulated in FMX. The loading capacities of each boron cluster derivative were determined via inductively-coupled plasma optical emission spectroscopy (ICP-OES) and kinetic analysis of release assumed first order release kinetics through dynamic dialysis. We found that most dodecaborate derivatives have similar release kinetics but have larger differences in their loading capacities. Finally, considering the ability of host-guest interactions to change properties such as solubility[13-16] and given the relevance of boron-rich compounds for boron neutron capture therapy (BNCT),[17] we have performed biodistribution experiments in mice to compare both free sodium dodecaborate (**1**) with sodium dodecaborate encapsulated in ferumoxytol (**1**@FMX). We find that **1**@FMX localizes in higher concentrations than free **1** at early time points and that the biodistribution and pharmacokinetics of **1**@FMX are similar to that of the BSH anion, a compound previously employed in several BNCT studies.[18,19] Overall, this work shows that boron clusters can be efficiently encapsulated into commercial polymer-based nanoparticle carriers, and this encapsulation can lead to altered biodistribution and pharmacokinetic properties in vivo.

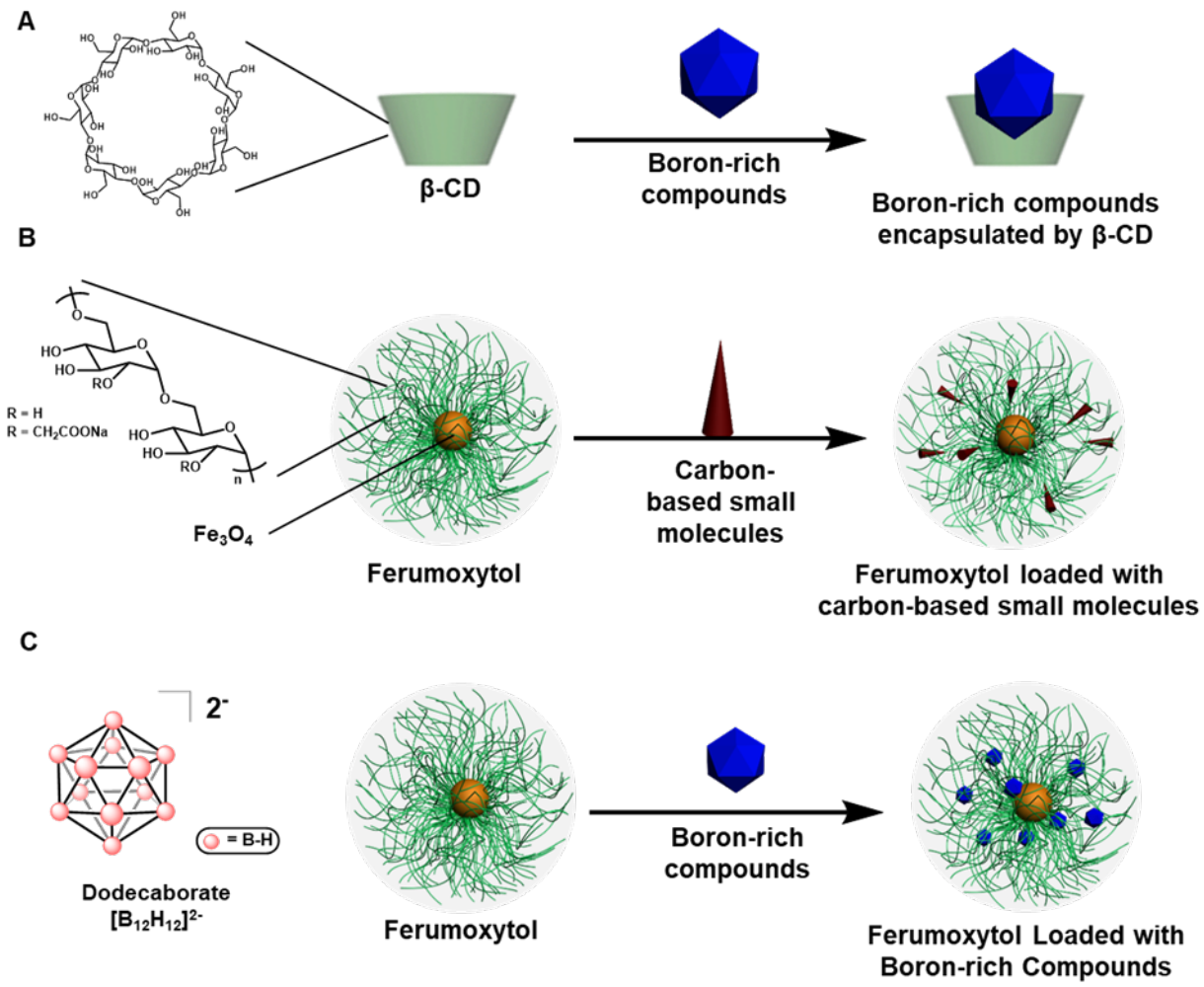

Figure 1. A) Previous work describing the encapsulation of boron-rich compounds with beta-cyclodextrin (β-CD).[3A] B) Previous work describing the encapsulation of carbon-based small molecules in ferumoxytol (FMX).[12] C) **This work**, the encapsulation of boron-rich compounds with ferumoxytol, a dextran-coated, iron oxide nanoparticle. The blue icosahedron represents various dodecaborate-based compounds and the red cone represents various carbon-based small molecules.

Experimental Section

Materials

All manipulations were performed at room temperature in laboratory air unless otherwise noted. Reagents were purchased from Sigma Aldrich, Oakwood Chemicals, TCI, Fisher Scientific, Boron Specialties, Acros Organics, Ricca Chemical, or Alfa Aesar, and used as received unless otherwise noted. Ferumoxytol (FMX) was obtained from AMAG Pharmaceuticals and was dialyzed and diluted to an Fe concentration of 1.8 mg/mL (confirmed by ICP-OES) prior to use.

Methods

All NMR spectra were obtained on a Bruker DRX 500 or Bruker Avance 400 broad band FT NMR spectrometers. ^{11}B chemical shifts were referenced to $BF_3 \bullet Et_2O$ (15% in $CDCl_3$, δ 0.0 ppm) unless otherwise stated. All ICP-OES data were obtained on an Agilent ICP-OES 5100 spectrometer. Samples were diluted in 4% HNO_3 using trace metal grade HNO_3 (Fisher) and LC-MS Grade water (Fisher). Standard solutions were prepared from commercially available 1000 ppm stock solutions of boron (Acros) and iron (Ricca Chemical). Standard addition using a 2 ppm yttrium stock solution was used for all samples. Plots and statistics (k, half-life, etc) for dynamic dialysis and biodistribution experiments were calculated using GraphPad Prism software.

Synthesis of FMX loaded with $Na_2B_{12}H_{12}$, 1 (1@FMX)

In a 1.5 mL Eppendorf tube, 100 mg of $Na_2B_{12}H_{12}$ (**1**) were added along with 100 μL Milli-Q H_2O. Then, 500 μL of FMX were added and the solution was mixed by shaking for 1 hour at room temperature. After mixing, the Eppendorf tube containing the solution was placed in a 5 °C fridge for 24 hrs. The solution was then transferred to a Pell Corp. 3 KDa MWCO centrifugal

filter device. 500 μL of Milli-Q H_2O was added and the solution was centrifuged at 3600 x*g* for 35 min. The addition of water followed by centrifugation was repeated twice for a total of 3 washes. Using ~100 μL of Milli-Q water, the solution was transferred to a clean Eppendorf tube and the solution volume was diluted to a total volume of 500 μL. Samples were stored in a 5 °C fridge and were vortexed prior to use.

Syntheses of FMX loaded with other compounds (general procedure)

In a 1.5 mL Eppendorf tube, 50 mg of boron cluster (**2-11**, see SI for synthetic details and references) were added along with 50 μL Milli-Q H_2O and 50 μL of DMSO. Then, 500 μL of FMX were added and the solution was mixed by shaking for 1 hour at room temperature. After mixing, the Eppendorf tube containing the solution was placed in a 5 °C fridge for 24 hrs. The solution was then filtered and transferred to a Pell Corp. 3 KDa MWCO centrifugal filter device. 500 μL of Milli-Q H_2O was added and the solution was centrifuged at 3600 x*g* for 35 min. The addition of water followed by centrifugation was repeated twice for a total of 3 washes. Using ~100 μL of Milli-Q water, the solution was transferred to a clean Eppendorf tube and the solution volume was diluted to a total volume of 500 μL. Samples were stored in a 5 °C fridge and were vortexed prior to use. Compound **11** caused precipitation of FMX and was not used further.

Static NMR Stability Experiments

In order to observe the potential leaching of boron under different conditions, solutions of FMX loaded with **1** were diluted with different reagents and NMR spectra were obtained. FMX was loaded with **1** following the general procedure, except the last dilution step to dilute the solution to a final volume of 500 μL used different reagent solutions other than water. The following

conditions were tested: neat Milli-Q H_2O, PBS 1x at pH 7.4, PBS 1x at pH 5.5, and 10% serum (FBS, 50 μL) in 1x minimum essential medium (MEM). 500 μL of each solution was placed into an NMR tube and a glass capillary filled with a ~400 mM solution of $B(OH)_3$ in D_2O was added as an internal standard. Room temperature ^{11}B NMR spectra (160 MHz, n=1024 scans) for each condition were collected at T= 1, 2, 4, and 24 hr. and intensities were normalized based on the peak corresponding to the $B(OH)_3$ internal standard ca. 20 ppm.

Dynamic Dialysis Experiments

FMX loaded with compounds following the above procedures were subjected to dynamic dialysis. 250 μL of each sample were added to a dialysis cup with a 20K MWCO. The dialysis cups were floated in 1 L of PBS pH 7.4 at 37 °C. Compound **1** was also measured in PBS at pH 5.5 and pH 10 as well as at pH 7.4 after a 2x dilution. At designated time points t = 1 h, 2 h, 4 h, and 6 h, 40 μL aliquots of sample were taken. An additional 40 μL aliquot of the initial sample was taken for a t = 0 h time point. Prior to ICP-OES analysis, each 40 μL aliquot was diluted to 10 mL with 4% HNO_3 (250x dilution, for Fe analysis) then 1 mL of the resulting solution was diluted to 10 mL with 4% HNO_3 (2500x dilution, for B analysis). Data were analyzed using GraphPad Prism to determine the first order leaching kinetic parameters. Boron content values were normalized and plotted as % of boron remaining over time. Several time points had a measured boron content too low to accurately quantify, resulting in incomplete data sets for several samples (**7**, **7b**, **10**, **11**).

Biodistribution Experiments

Biodistribution experiments using male BALB/c (n=3 per time point). All compounds were dosed at a concentration of 20 mg compound/kg in sterile PBS 1x pH 7.4. Mice were euthanized by CO_2 overdose at each time point and organs were collected by dissection. After removal, organs were

digested in trace metal grade concentrated nitric acid before being diluted prior to ICP-OES analysis. See Supporting Information for complete biodistribution experiment details and results.

Results and Discussion

Previously, researchers showed that mixing FMX nanoparticles with small molecules at mM concentrations can result in the association of small molecules with the corresponding polymer matrix.[12] Final loading concentrations were determined using either fluorescence emission or high performance liquid chromatography using standard curves. Initially, to commence our experiments and determine whether boron clusters can be efficiently encapsulated in ferumoxytol, we conducted a series of experiments with aqueous solutions of a sodium salt of an unfunctionalized *closo*-dodecahydrododecaborate ($Na_2B_{12}H_{12}$, **1**, 5 M) and commercial FMX (1.8 mg Fe/mL). By mixing aqueous solutions of both **1** and FMX at room temperature and using a centrifugal filter to remove excess dodecaborate, we recovered a red solution with no evidence of precipitation or sedimentation of the parent nanomaterial. Despite the superparamagnetic nature of the iron oxide core of FMX,[8] we were able to use NMR spectroscopy to probe the resulting nanoparticle solution and found that there was a strong, broad signal present in the ^{11}B NMR spectrum at -10 ppm (Figure 2). For comparison, the ^{11}B NMR signal of free **1** is ca. -15 ppm. The observation of only one ^{11}B NMR signal suggests that **1** remained intact and the broadening and location of the observed peak suggests that **1** is somehow associated with FMX nanoparticles. Additionally, using inductively coupled plasma optical emission spectroscopy (ICP-OES), we were able to quantify the boron content and found that boron loading was on the order of 10^4 boron clusters per FMX nanoparticle. To verify that the observed ^{11}B NMR chemical shift could indeed be assigned to encapsulated dodecaborate (**1**@FMX), an NMR titration was performed where a solution of **1** at 3.4 M was added in aliquots to a solution of FMX at 1.8 mg

Fe/mL and an NMR spectrum was obtained after the addition of each aliquot (Figure S1). At a concentration of **1** of 0.1 M, only the chemical shift corresponding to the encapsulated clusters (ca. -10 ppm) was observed, however, at higher boron cluster concentrations, the system appears to reach a saturation point where a second chemical shift corresponding to free dodecaborate (ca. -15 ppm) is also visible.

Analogous to the encapsulation of boron clusters in cyclodextrins (Figure 1A), we hypothesized that the carboxymethyl dextran polymer coating the surface of FMX would contain local pockets of dextran subunits that could bind various boron clusters. Encapsulation of carbon-based small molecules has been accomplished previously (Figure 1B) and we expected that boron clusters would behave similarly. Using **1** as an example, the lack of any covalent interactions between the boron cluster and FMX suggests there must be some noncovalent interactions responsible for the encapsulation. While chaotropism, as seen in the work by Assaf and coworkers, is a likely hypothesis for the encapsulation driving force, hydrogen bonding or ion pairing interactions are also possible and can be probed by evaluating the pH dependence of the system.

Having discovered that ^{11}B NMR spectroscopy was useful for the determination boron cluster encapsulation, we performed several stability studies (Figures S2, S3, S4, and S5) to assess the tolerance of the system to different pH values and media additives. Previously, a pH dependence has been seen in the release of carbon-based compounds from FMX as well as in the host-guest binding of small molecules in cyclodextrins and we therefore expected a pH dependence for the encapsulation equilibrium.[12,20] However, we found no change via ^{11}B NMR spectroscopy at low pH, high pH, or with the addition of fetal bovine serum and minimum essential medium. This further reinforces the hypothesis that hydrogen bonding or ion pairing interactions are less likely to be involved in the mechanism of encapsulation. The carboxymethyl dextran coating of FMX

contains several carboxylate groups that can be protonated or deprotonated as a function of pH. The change in available hydrogen bonding donor/acceptor sites or charged sites should have a measureable effect on release kinetics if these sites were involved in the encapsulation mechanism. The lack of pH dependence on release kinetics suggest some other phenomenon, such as chaotropism, is the likely driving force behind encapsulation.

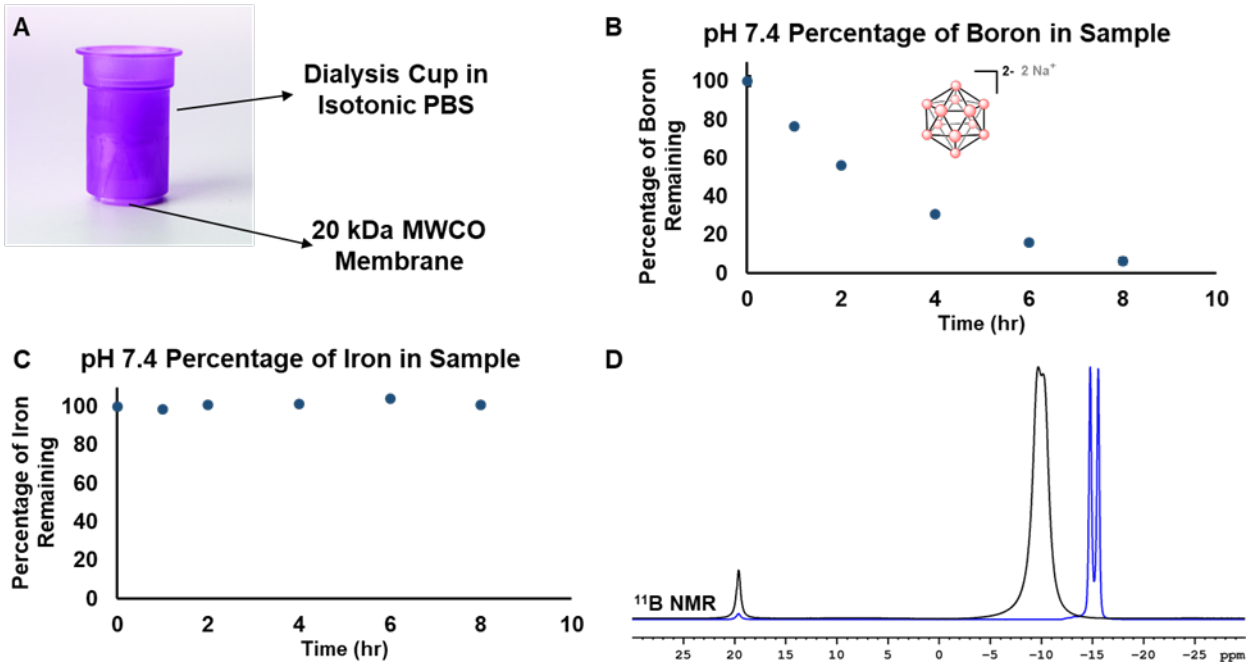

Figure 2. Overview of dynamic dialysis experiment used to determine kinetic parameters. (A) Dialysis cup used for experiments. The MWCO filter allows for the passage of free boron clusters but not ferumoxytol nanoparticles. (B) Decrease of boron content over time (measured by ICP-OES) as the boron clusters leach out of the ferumoxytol nanoparticles. (C) Retention of iron content over time (measured by ICP-OES) as the nanoparticles are retained in the dialysis cup. (D) ^{11}B NMR of free $Na_2B_{12}H_{12}$ (blue trace) as well as $Na_2B_{12}H_{12}$ encapsulated in ferumoxytol (black trace). Both spectra are referenced internally to $B(OH)_3$ ca. 20 ppm. Error bars show one standard deviation from measurement replicates.

Given that an NMR titration is a static system and that this technique might bias any release/encapsulation equilibrium, we further sought to validate our findings using a dynamic dialysis experiment. Using a dialysis cup with a molecular weight cut off (MWCO) membrane high enough to allow easy passage of dodecaborate derivatives but low enough to retain FMX nanoparticles, we quantified the amount of iron and boron over time using ICP-OES (Figure 2). Using **1**@FMX, we found that the amount of iron in solution remained constant, as expected, and that the boron content decreased over time following first order kinetics. We then repeated this experiment with phosphate buffered saline (PBS) at different pH values and also diluted the solution of **1**@FMX prior to dialysis. These changes had a minimal effect on release kinetics and first order half-lives for the release of **1** from FMX ranged from 2.0-2.4 hours (Figure 3). Even with the change from static to dynamic experiments, no significant pH dependence was detected. This further supports an alternative driving force to hydrogen bonding or ion pairing responsible for the attraction of boron clusters to FMX.

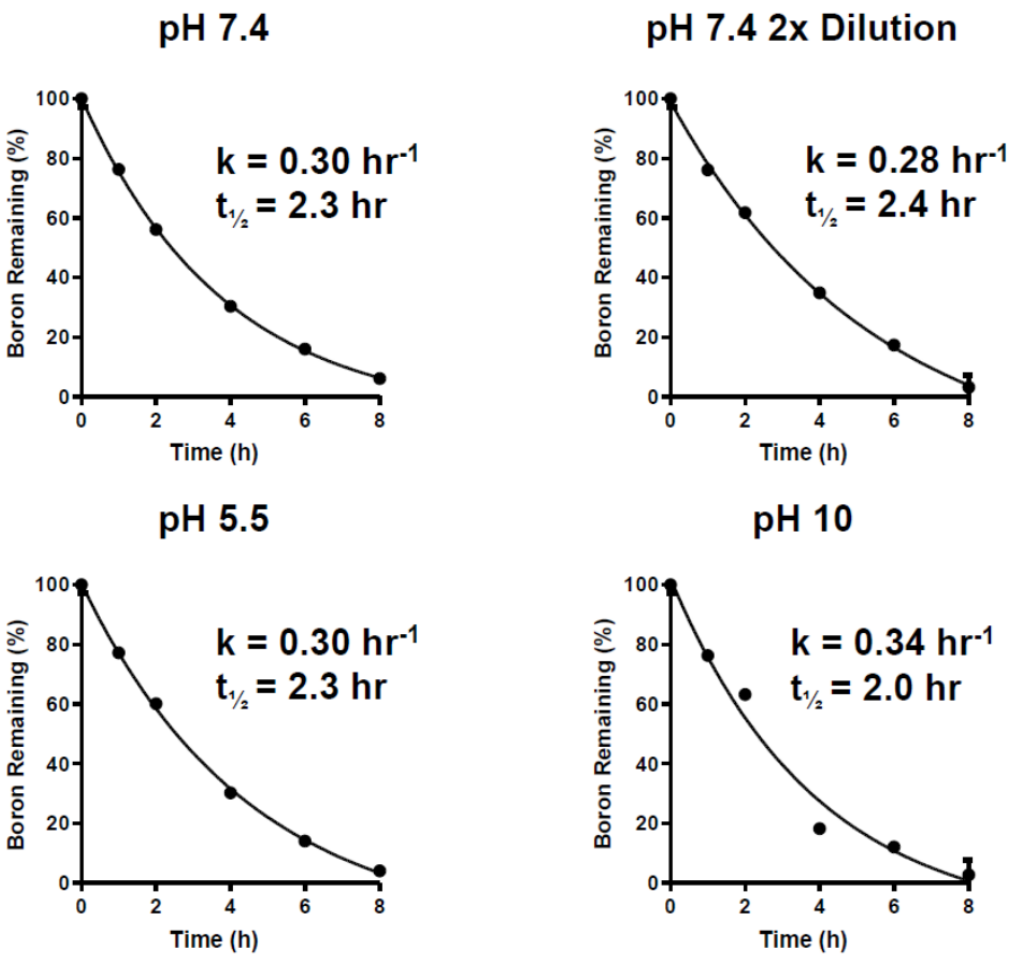

Figure 3. Dynamic dialysis results for the release of **1** from ferumoxytol in phosphate-buffered saline (PBS). Data were fitted to exponential decay trendlines to model first order release kinetics. Data were recorded as single trials with error bars showing one standard deviation from measurement replicates.

To further investigate what dictates the interaction between boron-rich clusters and FMX nanoparticles, we screened several dodecaborate derivatives containing a range of functional groups (Figure 4).[21-28] The compounds screened varied in charge, functional group, size, and cation. All kinetic analyses were measured in PBS at pH 7.4 for consistency and calculated kinetic parameters are recorded in Table 1. We found that the release half-lives ranged from 0.9-

2.6 hours and also found that most compounds resulted in similar boron concentrations after encapsulation. Compounds **7**, **7b**, and **10** had boron concentrations that were too low to accurately determine any kinetic parameters. Compound **11** induced precipitation so no kinetic parameters were determined. Structurally, **7**, **7b**, **10**, and **11** are relatively large compared to many of the other compounds tested. Both size and chemical structure are related to binding in analogous macromolecular systems and it could be that these compounds are too large for efficient binding. Additionally, the weak binding of **7** and **7b** suggests that hydrogen bonding is not likely involved in the binding of boron clusters and FMX. Both **7** and **7b** contain twelve hydroxyl groups that can act as both hydrogen bonding donors and acceptors and would likely facilitate strong binding if hydrogen bonding was the main driving force in this system.

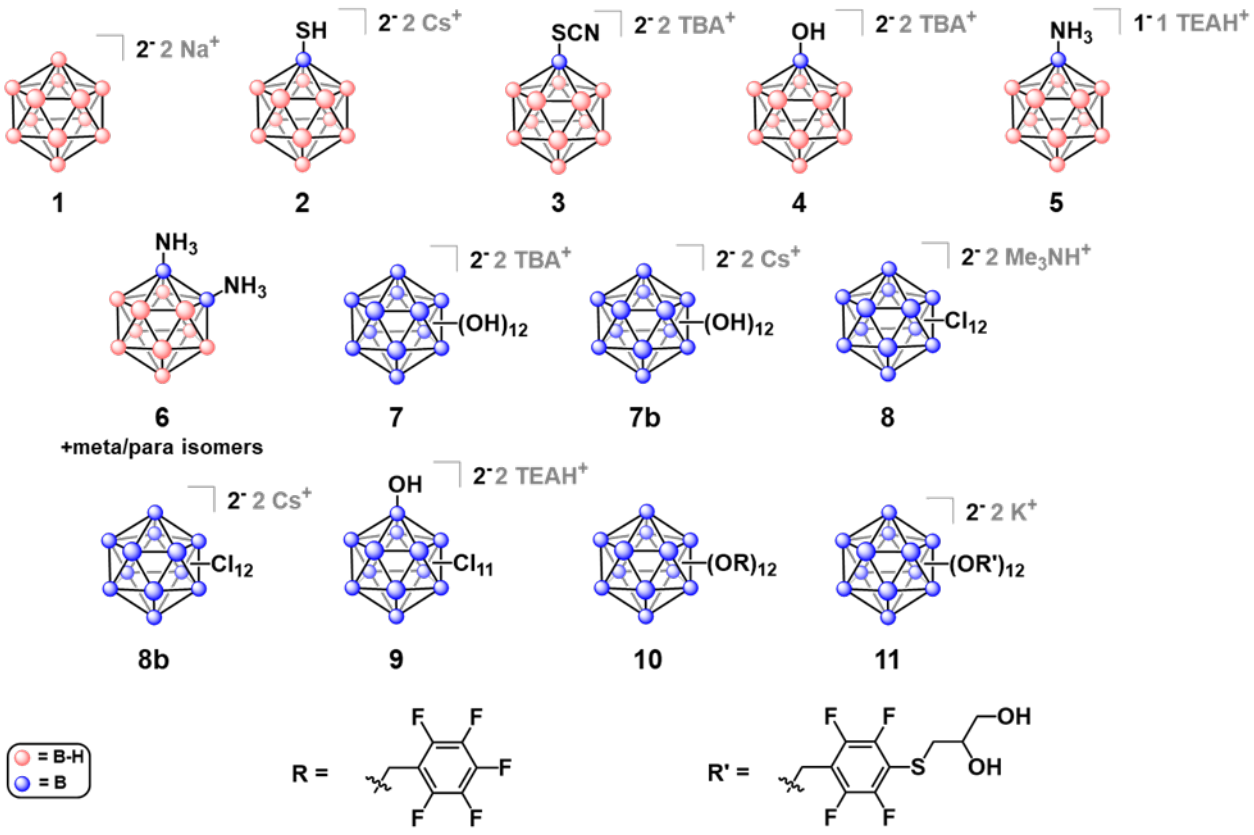

Figure 4. Dodecaborate derivatives screened. Kinetic data are shown in Table 1

Label	k (h^{-1})	$t_{½}$ (h)	Loading Efficiency
1	0.30	2.3	9.9%
2	0.22	3.2	49%
3	0.29	2.4	55%
4	0.21	3.3	3.4%
5	0.28	2.5	15%
6	0.30	2.3	6.3%
7*	---	---	17%
7b*	---	---	6.5%
8	0.30	2.3	67%
8b	0.34	2.0	87%
9	0.29	2.4	3.9%
10*	---	---	1.1%
11**	---	---	---

Table 1. Kinetic parameters from *in vitro* dynamic dialysis experiments. Compounds with no kinetic data had insufficient loading to determine their kinetic behavior. * insufficient retention to accurately determine kinetic parameters. ** induced precipitation during synthesis.

Given the ability of host-guest type interactions to alter properties such as solubility, we expected that sodium dodecaborate encapsulated in ferumoxytol would have an increased circulation time relative to free sodium dodecaborate and would thus alter biodistribution results. We therefore compared the biodistribution in BALB/c mice of free sodium dodecaborate (**1**), sodium dodecaborate encapsulated in ferumoxytol (**1**@FMX). Cs_2BSH (**2**) was used as a non-

encapsulated positive control given that it was previously shown to localize in multiple organs due to its propensity to associate with serum proteins.[29] Given the historical relevance of **2** to BNCT, this compound served as a benchmark for our study. Mice were injected via intraperitoneal (IP) injection and all compounds were dosed at 20 mg/kg. Mice were sacrificed at time points from 0 hr to 24 hr at which point the major organs were harvested and boron content was determined using ICP-OES. Importantly, throughout the duration of the study, no mice developed any visible adverse effects, suggesting that these boron cluster formulations are non-toxic to mice. Select biodistribution data is summarized in Figure 5 and the complete biodistribution is in the SI. Consistent with our original hypothesis, we found that at early time points, **1**@FMX had the highest detected boron values in multiple organs and serum, relative to free **1** or **2**. Consistent with in vitro release kinetics, in vivo results show similar timescales with little boron detected after 8 hours. Interestingly, less than 1 μg B per g tissue was detected in the brain for all studied formulations, suggesting that neither **1** nor **2** significantly cross the blood-brain barrier in healthy mice at the injected concentrations. Similarly, encapsulation of **1** with FMX does not increase the concentration of boron in the brain. In contrast, in the lungs, heart, spleen, liver, kidneys, and serum, **1**@FMX showed higher boron concentrations up to 2-fold compared to **1** or **2**. In the lungs, heart, spleen, liver, kidneys, and serum, **1**@FMX reached concentrations of 24, 7, 66, 32, 21, and 40 μg B per g tissue, respectively. Retention also varied in different organs with the spleen and heart showing very low retention relative to the liver, lungs, kidneys, and serum. These results indicate that the chaotropic encapsulation of molecules into a polymeric nanoparticle-based carrier can significantly change the biodistribution of the corresponding guest in mice.

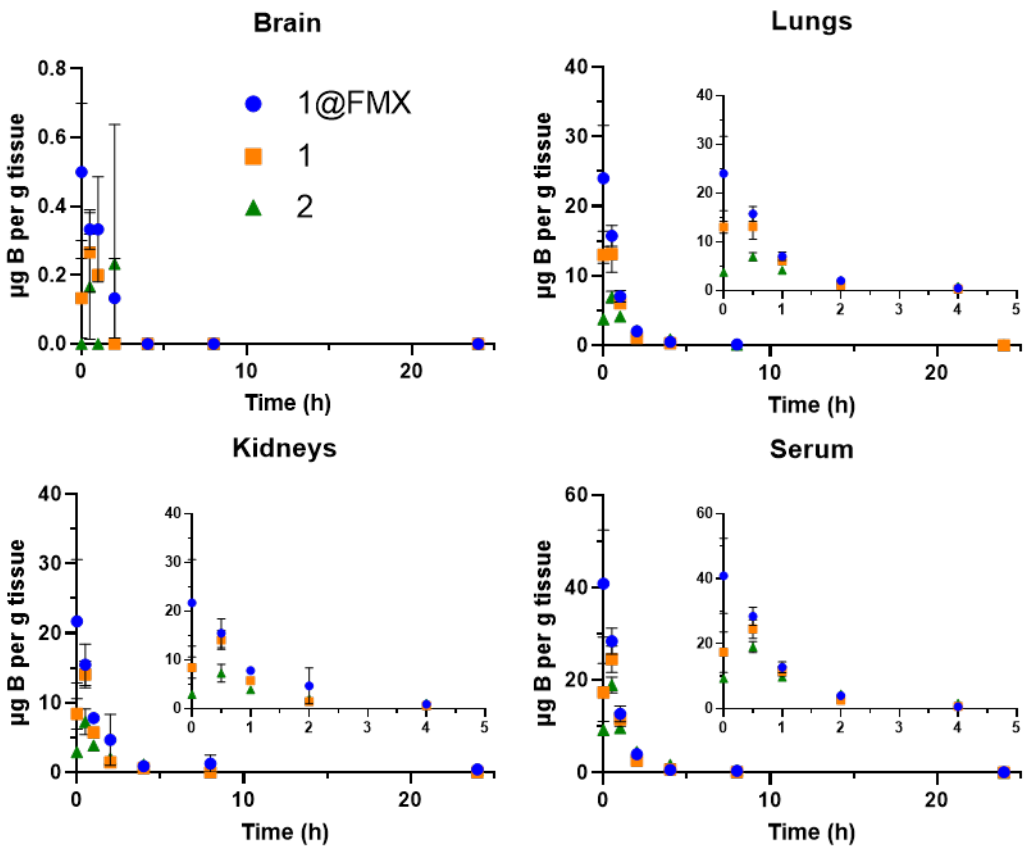

Figure 5. Biodistribution of ferumoxytol-encapsulated **1** (**1**@FMX, blue circles) compared to **1** (orange squares) alone and **2** (green triangles) in selected organs. Boron content was measured via ICP-OES and is reported as mass of boron per gram of wet tissue. All values were measured in triplicate and error bars show one standard deviation. Please see the Supporting Information for more experimental details as well as the complete biodistribution data. The inset on each graph shows the first 5 time points.

Summary and Conclusions

We report the successful encapsulation of several dodecaborate derivatives into ferumoxytol nanoparticles and have determined their release kinetics. While previous work has shown that boron clusters can associate strongly with cyclodextrins and several other well-defined

macrocyclic guest molecules, we demonstrate that dodecaborate derivatives also can associate with the carboxylated dextran polymer matrix in ferumoxytol and have first order release half-lives on the order of hours. We evaluated the effects of encapsulation with a biodistribution study comparing our system with free boron cluster and found that the encapsulated system **1**@FMX increases absorption of **1** into several organs in BALB/c mice. At a dose of 20 mg/kg, **1**@FMX localized in tissues ranging from 0-65 μg B per g tissue, suggesting that encapsulation of dodecaborate-based compounds in a polymer matrix can potentially have favorable effects on biodistribution results. More broadly, this work suggests the potential importance of non-covalent interaction between boron clusters and polymers stemming from non-electrostatic interactions and points to new avenues for creating hybrid boron-cluster based nanomaterials without covalent attachment.[30]

ASSOCIATED CONTENT

The following files are available free of charge.

Additional experimental details and data (PDF)

AUTHOR INFORMATION

Corresponding Author

*Email: jmanuel.perez@nih.gov

*Email: spokoyny@chem.ucla.edu

Present Addresses

†J.M.P.: National Cancer Institute, 9000 Rockville Pike, Bethesda, MD 20892

Notes

The authors declare the following competing financial interest: J. M. P., A. M. S., J. T., and N. A. B. are inventors on the patent application WO2019204645A1 disclosing this and related work.

ACKNOWLEDGMENT

The authors acknowledge the financial support of TAE Life Sciences. We also thank researchers at TAE Life Sciences, especially Dr. Kendall Morrison, Dr. Art Raitano, and Dr. Michael Torgov. The authors thank Agilent Technologies, Inc. for the generous loan of ICP-OES 5100 instrumentation, UCLA Division of Laboratory Animal Medicine (DLAM) and Dr. Alice Soragni (UCLA) for assistance with the mouse studies, and the staff at the UCLA Molecular Instrumentation Center (MIC) for help with NMR spectroscopy. Synthesis of compounds **2**-**11** was supported by NIGMS MIRA award (R35GM124746) to A. M. S.

REFERENCES

1. Wagner, B. D. *Host–Guest Chemistry*; De Gruyter: Berlin, Boston, 2020.

2. Recent representative examples and reviews: A) Geng, W. C.; Sessler, J. L.; Guo, D. S. Supramolecular Prodrugs Based on Host-Guest Interactions. *Chem. Soc. Rev.* **2020**, *49* (8), 2303–2315. B) Wenz, G. An Overview of Host-Guest Chemistry and Its Application to Nonsteroidal Anti-Inflammatory Drugs. *Clin. Drug Investig.* **2000**, *19*, 21–25. C) Yu, G.; Chen, X. Host–Guest Chemistry in Supramolecular Theranostics. *Theranostics* **2019**, *9* (11), 3041–3074. D) Qu, D. H.; Wang, Q. C.; Zhang, Q. W.; Ma, X.; Tian, H. Photoresponsive Host-Guest Functional Systems. *Chem. Rev.* **2015**, *115* (15), 7543–7588. E) Teyssandier, J.; Feyter, S. De; Mali, K. S. Host-Guest Chemistry in Two-Dimensional Supramolecular Networks. *Chem. Commun.* **2016**, *52* (77), 11465–11487.

3. A) Assaf, K. I.; Ural, M. S.; Pan, F.; Georgiev, T.; Simova, S.; Rissanen, K.; Gabel, D.; Nau, W. M. Water Structure Recovery in Chaotropic Anion Recognition: High-Affinity Binding of Dodecaborate Clusters to γ-Cyclodextrin. *Angew. Chem. Int. Ed.* **2015**, *54*, 6852–6856. B) Assaf, K. I.; Suckova, O.; Al Danaf, N.; von Glasenapp, V.; Gabel, D.; Nau, W. M. Dodecaborate-Functionalized Anchor Dyes for Cyclodextrin-Based Indicator Displacement Applications. *Org. Lett.* **2016**, *18*, 932–935. C) Assaf, K. I.; Gabel, D.; Zimmermann, W.; Nau, W. M. High-affinity host–guest chemistry of large-ring cyclodextrins. *Org. Biomol. Chem.* **2016**, *14*, 7702–7706. D) Warneke, J.; Jenne, C.; Bernarding, J.; Azov, V. A.; Plaumann, N. Evidence for an intrinsic binding force between dodecaborate dianions and receptors with hydrophobic binding pockets. *Chem. Commun.* **2016**, *52*, 6300–6303. E) Messina, M. S.; Graefe, C. T.; Chong, P.; Ebrahim, O. M.; Pathuri, R. S.; Bernier, N. A.; Mills, H. A.; Rheingold, A. L.; Frontiera, R. R.; Maynard, H. D.; Spokoyny, A. M. Carborane RAFT agents as tunable and functional molecular probes for polymer materials. *Polym. Chem.* **2019**, *10*, 1660–1667. F) Waddington, M. A.; Zheng, X.; Stauber, J. M.; Hakim Moully, E.; Montgomery, H. R.; Saleh, L. M. A.; Král, P.; Spokoyny, A. M. An Organometallic Strategy for Cysteine Borylation. *J. Am. Chem. Soc.* **2021**, *143* (23), 8661–8668.

4. Wang, W.; Wang, X.; Cao, J.; Liu, J.; Qi, B.; Zhou, X.; Zhang, S.; Gabel, D.; Nau, W. M.; Assaf, K. I.; Zhang, H. The chaotropic effect as an orthogonal assembly motif for multi-responsive dodecaboratecucurbituril supramolecular networks. *Chem. Commun.* **2018**, *54*, 2098–2101.

5. Karki, K.; Gabel, D.; Roccatano, D. Structure and Dynamics of Dodecaborate Clusters in Water. *Inorg. Chem.* **2012**, *51*, 4894–4896.

6. Kataki-Anastasakou, A.; Axtell, J. C.; Hernandez, S.; Dziedzic, R. M.; Balaich, G. J.; Rheingold, A. L.; Spokoyny, A. M.; Sletten, E. M. Carborane Guests for Cucurbit[7]Uril Facilitate Strong Binding and On-Demand Removal. *J. Am. Chem. Soc.* **2020**, *142* (49), 20513–20518.

7. Li, J.; Janoušková, O.; Fernandez-Alvarez, R.; Mesíková, S.; Tošner, Z.; Kereïche, S.; Uchman, M.; Matějíček, P. Designed Boron-Rich Polymeric Nanoparticles Based on Nano-Ion Pairing for Boron Delivery. *Chem. Eur. J.* **2020**, *26* (63), 14283–14289.

8. A) Bullivant, J. P.; Zhao, S.; Willenberg, B. J.; Kozissnik, B.; Batich, C. D.; Dobson, J. Materials Characterization of Feraheme/Ferumoxytol and Preliminary Evaluation of Its Potential for Magnetic Fluid Hyperthermia. *Int. J. Mol. Sci.* **2013**, *14*, 17501–17510. B) Bryant, L. H.; Kim, S. J.; Hobson, M.; Milo, B.; Kovacs, Z. I.; Jikaria, N.; Lewis, B. K.; Aronova, M. A.; Sousa, A. A.; Zhang, G.; Leapman, R. D.; Frank, J. A. Physicochemical Characterization of Ferumoxytol, Heparin and Protamine Nanocomplexes for Improved Magnetic Labeling of Stem Cells. *Nanomedicine Nanotechnology, Biol. Med.* **2017**, *13* (2), 503–513.

9. Hildebrandt, N.; Hermsdorf, D.; Signorell, R.; Schmitz, S. A.; Diederichsen, U. Superparamagnetic iron oxide nanoparticles functionalized with peptides by electrostatic interactions. *Arkvoc* **2007**, *5*, 79–90.

10. Yu, M. K.; Jeong, Y. Y.; Park, J.; Park, S.; Kim, J. W.; Min, J. J.; Kim, K.; Jon, S. Drug-Loaded Superparamagnetic Iron Oxide Nanoparticles for Combined Cancer Imaging and Therapy In Vivo. *Angew. Chem. Int. Ed.* **2008**, *47*, 5362–5365.

11. Santra, S.; Kaittanis, C.; Grimm, J.; Perez, J. M. Drug/Dye-Loaded, Multifunctional Iron Oxide Nanoparticles for Combined Targeted Cancer Therapy and Dual Optical/Magnetic Resonance Imaging. *Small* **2009**, *5*, 1862–1868.

12. Kaittanis, C.; Shaffer, T. M.; Ogirala, A.; Santra, S.; Perez, J. M.; Chiosis, G.; Li. Y.; Josephson, L.; Grimm, J. Environment-responsive nanophores for therapy and treatment monitoring via molecular MRI quenching. *Nat. Commun.* **2014**, *5*, 3384.

13. Liu, Y.; Chen, G.-S.; Li, L.; Zhang, H.-Y.; Cao, D.-X.; Yuan, Y-J. Inclusion Complexation and Solubilization of Paclitaxel by Bridged Bis(β-cyclodextrin)s Containing a Tetraethylenepentaamino Spacer. *J. Med. Chem.* **2003**, *46*, 4634–4637.

14. Edwards, W. B.; Reichert, D. E.; d'Avignon, D. A.; Welch, M. J. β-Dyclodextrin dimers as potential tumor pretargeting agents. *Chem. Commun.* **2001**, *14*, 1312–1313.

15. Ruebner, A.; Yang, Z.; Leung, D.; Breslow, R. A cyclodextrin dimer with a photocleavable linker as a possible carrier for the photosensitizer in photodynamic tumor therapy. *Proc. Natl. Acad. Sci.* **1999**, *96*, 14692–14693.

16. Yong, J.-H.; Barth, R. F.; Rotaru, J. H.; Wyzlic, I. M.; Soloway, A. H. Evaluation of *in Vitro* Cytotoxicity of Carboranyl Amino Acids, their Chemical Precursors and *nido* Carboranyl Amino Acids for Boron Neutron Capture Therapy. *Anticancer Res.* **1995**, *15*, 2039–2044.

17. Hawthorne, M. F.; Lee, M. W. A critical assessment of boron target compounds for boron neutron capture therapy. *J. Neuro-Oncol.* **2003**, *62*, 33–45.

18. Barth, R. F.; Mi, P.; Yang, W. Boron Delivery Agents for Neutron Capture Therapy of Cancer. *Cancer Commun*. **2018**, *38* (1), 1–15.

19. Lamba, M.; Goswami, A.; Bandyopadhyay, A. A Periodic Development of BPA and BSH Based Derivatives in Boron Neutron Capture Therapy (BNCT). *Chem. Commun*. **2021**, *57* (7), 827–839.

20. Samuelsen, L.; Holm, R.; Lathuile, A.; Schönbeck, C. Correlation between the stability constant and pH for β-cyclodextrin complexes. *Int. J. Pharm*. **2019**, *568*, 118523.

21. Geis, V.; Guttsche, K.; Knapp, C.; Scherer, H.; Uzun, R. Synthesis and Characterization of Synthetically Useful Salts of the Weakly-Coordinating Dianion $[B_{12}Cl_{12}]^{2-}$. *Dalton Trans*. **2009**, 2687–2694.

22. Tolpin, E. I.; Wellum, G. R.; Berley, S. A. Synthesis and chemistry of mercaptoundecahydro-closo-dodecaborate(2-). *Inorg. Chem*. **1978**, *17*, 2867–2873.

23. Lepšík, M.; Srnec, M.; Plešek, J.; Buděšínský, M.; Klepetářová, B.; Hnyk, D.; Grüner, B.; Rulíšek, L. Thiocyanation of *closo*-Dodecaborate $B_{12}H_{12}^{2-}$. A Novel Synthetic Route and Theoretical Elucidation of the Reaction Mechanism. *Inorg. Chem*. **2010**, *49*, 5040–5048.

24. Peymann, T.; Knobler, C. B.; Hawthorne, M. F. A Study of the Sequential Acid-Catalyzed Hydroxylation of Dodecahydro-*closo*-dodecaborate(2–). *Inorg Chem*. **2000**, *39*, 1163–1170.

25. Zhang, Y.; Liu, J.; Duttwyler, S. Synthesis and Structural Characterization of Ammonio/Hydroxo Undecachloro-*closo*-Dodecaborates $[B_{12}Cl_{11}NH_3]/[B_{12}Cl_{11}OH]^{2-}$ and Their Derivatives. *Eur. J. Inorg. Chem.* **2015**, *2015*, 5158–5162.

26. Pluntze, A. M.; Bukovsky, E. V.; Lacroix, M. R.; Newell, B. S.; Rithner, C. D.; Strauss, S. H. Deca-*B*-fluorination of diammonioboranes. Structures and NMR characterization of 1,2-, 1,7-, and 1,12-$B_{12}H_{10}(NH_3)_2$ and 1,2-, 1,7-, and 1,12-$B_{12}F_{10}(NH_3)_2$. *J. Fluor. Chem.* **2018**, *209,* 33–42.

27. Qian, E. A.; Wixtrom, A. I.; Axtell, J. C.; Saebi, A.; Jung, D.; Rehak, P.; Han, Y.; Moully, E. H.; Mosallaei, D.; Chow, S.; Messina, M.; Wang, J.-Y.; Royappa, A. T.; Rheingold, A. L.; Maynard, H. D.; Kral, P.; Spokoyny, A. M. Atomically Precise Organomimetic Cluster Nanomolecules Assembled via Perfluoroaryl-Thiol S_NAr Chemistry. *Nature Chem.* **2017**, *9*, 333–340.

28. Gu, W.; Ozerov, O. V. Exhaustive Chlorination of $[B_{12}H_{12}]^{2-}$ without Chlorine Gas and the Use of $[B_{12}Cl_{12}]^{2-}$ as a Supporting Anion in Catalytic Hydrodefluorination of Aliphatic C-F Bonds. *Inorg. Chem.* **2011**, *50*, 2726–2728.

29. Soloway, A. H.; Hatanaka, H.; Davis, M. A. Penetration of Brain and Brain Tumor. V II. Tumor-Binding Sulfhydryl Boron Compounds. *J. Med. Chem.* **1967**, *10* (4), 714–717.

30. A) Matějíček, P.; Cígler, P.; Olejniczak, A. B.; Andrysiak, A.; Wojtczak, B.; Procházka, K.; Lesnikowski, Z. J. Aggregation Behavior of Nucleoside-Boron Cluster Conjugates in Aqueous Solutions. *Langmuir* **2008**, *24* (6), 2625–2630. B) Yan, J.; Yang, W.; Zhang, Q.; Yan, Y. Introducing Borane Clusters into Polymeric Frameworks: Architecture, Synthesis,

and Applications. *Chem. Commun.* **2020**, *56* (79), 11720–11734. C) Pitto-Barry, A. Polymers and Boron Neutron Capture Therapy (BNCT): A Potent Combination. *Polym. Chem.* **2021**, *12* (14), 2035–2044. D) Fernandez-Alvarez, R.; Ďorďovič, V.; Uchman, M.; Matějíček, P. Amphiphiles without Head-and-Tail Design: Nanostructures Based on the Self-Assembly of Anionic Boron Cluster Compounds. *Langmuir* **2018**, *34* (12), 3541–3554. E) Rossi, S.; Karlsson, G.; Martini, G.; Edwards, K. Combined Cryogenic Transmission Electron Microscopy and Electron Spin Resonance Studies of Egg Phosphatidylcholine Liposomes Loaded with a Carboranyl Compound Intended for Boron Neutron Capture Therapy. *Langmuir* **2003**, *19* (14), 5608–5617. F) Ďorďovič, V.; Tošner, Z.; Uchman, M.; Zhigunov, A.; Reza, M.; Ruokolainen, J.; Pramanik, G.; Cígler, P.; Kalíková, K.; Gradzielski, M.; Matějíček, P. Stealth Amphiphiles: Self-Assembly of Polyhedral Boron Clusters. *Langmuir* **2016**, *32* (26), 6713–6722. G) Ban, H. S.; Nakamura, H. Recent Development of Nanoparticle-Based Boron Delivery Systems for Neutron Capture Therapy. In *Handbook of Boron Science*; WORLD SCIENTIFIC (EUROPE), 2018; pp 49–68. H) Takagaki, M.; Kazuko, U.; Hosmane, N. S. An Overview of Clinical and Biological Aspects of Current Boron Neutron Capture Therapy (BNCT) for Cancer Treatment. In *Handbook of Boron Science*; WORLD SCIENTIFIC (EUROPE), 2018; pp 101–143. I) Das, B. C.; Ojha, D. P.; Das, S.; Hosmane, N. S.; Evans, T. Boron Compounds for Molecular Probes and Therapeutics. In *Handbook of Boron Science*; WORLD SCIENTIFIC (EUROPE), 2018; pp 145–165. J) Chauhan, N. P. S.; Hosmane, N. S.; Mozafari, M. Boron-Based Polymers: Opportunities and Challenges. *Mater. Today Chem.* **2019**, *14*, 100184. K) Zhu, Y.; Hosmane, N. S. Advanced Carboraneous Materials. *J. Organomet. Chem.* **2017**, *849–850*, 286–292. L) Assaf, K. I.; Wilińska, J.; Gabel, D. Ionic

Boron Clusters as Superchaotropic Anions. *Boron-Based Compounds*. April 24, 2018, pp 109–125. M) Viñas Teixidor, C.; Teixidor, F.; Harwood, A. J. Cobaltabisdicarbollide-Based Synthetic Vesicles. *Boron-Based Compounds*. April 24, 2018, pp 159–173. N) Sivaev, I. B.; Anufriev, S. A.; Suponitsky, K. Y.; Godovikov, I. A.; Bregadze, V. I. Intramolecular Non-Covalent Interactions in Nido-Carboranes and Metallacomplexes. *Phosphorus, Sulfur Silicon Relat. Elem.* **2018**, *193* (2), 104–109. O) Bregadze, V. I.; Sivaev, I. B.; Dubey, R. D.; Semioshkin, A.; Shmal'ko, A. V.; Kosenko, I. D.; Lebedeva, K. V.; Mandal, S.; Sreejyothi, P.; Sarkar, A.; Shen, Z.; Wu, A.; Hosmane, N. S. Boron-Containing Lipids and Liposomes: New Conjugates of Cholesterol with Polyhedral Boron Hydrides. *Chem. Eur. J.* **2020**, *26* (61), 13832–13841. P) Guerrero, I.; Saha, A.; Xavier, J. A. M.; Viñas, C.; Romero, I.; Teixidor, F. Noncovalently Linked Metallacarboranes on Functionalized Magnetic Nanoparticles as Highly Efficient, Robust, and Reusable Photocatalysts in Aqueous Medium. *ACS Appl. Mater. Interfaces* **2020**, *12* (50), 56372–56384. Q) Oleshkevich, E.; Morancho, A.; Saha, A.; Galenkamp, K. M. O.; Grayston, A.; Crich, S. G.; Alberti, D.; Protti, N.; Comella, J. X.; Teixidor, F.; Rosell, A.; Viñas, C. Combining Magnetic Nanoparticles and Icosahedral Boron Clusters in Biocompatible Inorganic Nanohybrids for Cancer Therapy. *Nanomedicine Nanotechnology, Biol. Med.* **2019**, *20*, 101986. R) Oleshkevich, E.; Teixidor, F.; Rosell, A.; Viñas, C. Merging Icosahedral Boron Clusters and Magnetic Nanoparticles: Aiming toward Multifunctional Nanohybrid Materials. *Inorg. Chem.* **2018**, *57* (1), 462–470. S) Ching, H. Y. V.; Clarke, R. J.; Rendina, L. M. Supramolecular β-Cyclodextrin Adducts of Boron-Rich DNA Metallointercalators Containing Dicarba-Closo-Dodecaborane(12). *Inorg. Chem.* **2013**, *52* (18), 10356–10367. T) Ching, H. Y. V.; Clifford, S.; Bhadbhade, M.; Clarke, R. J.;

Rendina, L. M. Synthesis and Supramolecular Studies of Chiral Boronated Platinum(Ii) Complexes: Insights into the Molecular Recognition of Carboranes by β-Cyclodextrin. *Chem. - A Eur. J.* **2012**, *18* (45), 14413–14425. U) Nakamura, H. Boron Lipid-Based Liposomal Boron Delivery System for Neutron Capture Therapy: Recent Development and Future Perspective. *Future Med. Chem.* **2013**, *5* (6), 715–730. V) Tachikawa, S.; Miyoshi, T.; Koganei, H.; El-Zaria, M. E.; Viñas, C.; Suzuki, M.; Ono, K.; Nakamura, H. Spermidinium Closo-Dodecaborate-Encapsulating Liposomes as Efficient Boron Delivery Vehicles for Neutron Capture Therapy. *Chem. Commun.* **2014**, *50* (82), 12325–12328. W) Chan, W. J.; Cho, H. L.; Goudar, V.; Bupphathong, S.; Shu, C. H.; Kung, C.; Tseng, F. G. Boron-Enriched Polyvinyl-Alcohol/Boric-Acid Nanoparticles for Boron Neutron Capture Therapy. *Nanomedicine* **2021**, *16* (6), 441–452. X) Yamana, K.; Kawasaki, R.; Sanada, Y.; Tabata, A.; Bando, K.; Yoshikawa, K.; Azuma, H.; Sakurai, Y.; Masunaga, S. ichiro; Suzuki, M.; Sugikawa, K.; Nagasaki, T.; Ikeda, A. Tumor-Targeting Hyaluronic Acid/Fluorescent Carborane Complex for Boron Neutron Capture Therapy. *Biochem. Biophys. Res. Commun.* **2021**, *559*, 210–216.

Table of Contents (TOC) Graphical Abstract: